DDB1-Mediated CRY1 Degradation Promotes FOXO1-Driven Gluconeogenesis in Liver

Xin Tong, Deqiang Zhang, Nicholas Charney, Ethan Jin, Kyle VanDommelen, Kenneth Stamper, Neil Gupta, Johnny Saldate, and Lei Yin

Targeted protein degradation through ubiquitination is an important step in the regulation of glucose metabolism. Here, we present evidence that the DDB1-CUL4A ubiquitin E3 ligase functions as a novel metabolic regulator that promotes FOXO1-driven hepatic gluconeogenesis. In vivo, hepatocyte-specific *Ddb1* deletion leads to impaired hepatic gluconeogenesis in the mouse liver but protects mice from high-fat diet–induced hyperglycemia. Lack of *Ddb1* downregulates FOXO1 protein expression and impairs FOXO1-driven gluconeogenic response. Mechanistically, we discovered that DDB1 enhances FOXO1 protein stability via degrading the circadian protein cryptochrome 1 (CRY1), a known target of DDB1 E3 ligase. In the *Cry1* depletion condition, insulin fails to reduce the nuclear FOXO1 abundance and suppress gluconeogenic gene expression. Chronic depletion of *Cry1* in the mouse liver not only increases FOXO1 protein but also enhances hepatic gluconeogenesis. Thus, we have identified the DDB1-mediated CRY1 degradation as an important target of insulin action on glucose homeostasis.

Maintaining steady levels of glucose is crucial for the survival and health of mammals during feeding and fasting cycles. During fasting, the liver serves as the major site to keep blood glucose steady by activating de novo gluconeogenesis. During feeding, insulin reduces the glucose surge by promoting glycogen synthesis while inhibiting gluconeogenesis in the liver (1–3). The hepatic insulin signaling cascade has been shown to be indispensable in maintaining glucose homeostasis in animal models. Mice lacking insulin receptors in hepatocytes quickly develop hyperglycemia and hyperinsulinemia independently of obesity (4). In patients with diabetes, severe hepatic insulin resistance has been considered to be a major driver in excessive hepatic glucose production and fasting-associated hyperglycemia (2). Therefore, the ability of insulin to suppress hepatic glucose production has been targeted to treat diabetes.

Previous studies have established FOXO1 as a key transcription factor in integrating insulin signaling and hepatic glucose metabolism (5,6). Under normal physiological conditions, insulin activates the phosphatidylinositol 3-kinase–AKT pathway, which in turn phosphorylates the transcription factor FOXO1 at T24/S253/S316 (7). Subsequently, phosphorylated FOXO1 is excluded from the nucleus, leading to reduced mRNA levels of key gluconeogenic enzymes such as *G6pase* (glucose-6-phosphatase) and *Pepck* (phosphoenolpyruvate carboxykinase) (8–11). However, in the case of insulin resistance, the nuclear accumulation of FOXO1 promotes transcription of gluconeogenic enzymes and eventually results in hyperglycemia (12,13). FOXO1 has been found to be targeted for proteasomal degradation via ubiquitination downstream of insulin signaling (14–16). Several E3 ligases including MDM2, SKP2, and COP1 promote FOXO1 ubiquitination and degradation at least in vitro (17–19). Since inactivation of FOXO1 transcriptional activity is the major route for insulin to inhibit gluconeogenesis, inhibition of FOXO1-mediated gluconeogenesis by targeting its degradation could offer a promising avenue to treat diabetes without activating the insulin-AKT–dependent lipogenic pathway.

DDB1 (DNA-damage–binding protein 1) is a scaffolding component of the DDB1-CUL4A ubiquitin E3 ligase complex (20–22). Within this complex, DDB1 serves as the linker protein between CUL4A and substrate-binding proteins (21,23). *Ddb1* deletion disrupts the DDB1-CUL4A complex and subsequently abolishes its E3 ligase actions (21,24,25). DDB1-CUL4A E3 ligase promotes ubiquitination and degradation

METABOLISM

of a variety of substrates, including p27, c-JUN, and CDT1 (23,26,27). We recently discovered that DDB1-CUL4A E3 ligase targets CRY1 for ubiquitination and degradation via DDB1 and CUL4-associated factors (DCAF) protein CDT2 (28). *Ddb1* deletion increases total levels of CRY1 protein in mouse hepatocytes and mouse liver. Thus far, the role of DDB1 in liver metabolism is largely unknown, since *Ddb1* global knockout is embryonically lethal (24). Given the emerging role of CRY1 in liver metabolism (29,30), it is likely that DDB1 could function as a metabolic regulator at least by manipulating the CRY1 protein stability.

CRY1 is an evolutionarily conserved clock protein with diverse functions (31). Besides its classic function as a negative regulator of the circadian network, CRY1 has been shown to be a novel regulator of glucose metabolism. Ectopic overexpression of CRY1 in liver reverses hyperglycemia in *db/db* mice, a type 2 diabetes model, by interfering with CREB-dependent glucagon signaling (30). CRY1 was also found to modulate glucocorticoid receptor function during the induction of gluconeogenesis (29). Recently, SREBP-1c–induced *Cry1* has been shown to regulate hepatic glucose production (32). All these studies have highlighted the critical role of CRY1 in hepatic glucose metabolism under both normal and pathological conditions.

In this study, we examined the role of DDB1 E3 ligase in hepatic glucose metabolism. We established for the first time that DDB1 E3 ligase is a novel positive regulator of hepatic gluconeogenesis. Hepatocyte deficiency of *Ddb1* not only suppresses hepatic gluconeogenesis during fasting but also protects mice from high-fat diet (HFD)-induced fasting hyperglycemia. At the mechanistic level, DDB1 increases FOXO1 protein via CRY1 degradation and promotes the FOXO1-driven gluconeogenesis in hepatocytes. In *Cry1*-depleted hepatocytes, insulin fails to reduce nuclear FOXO1 abundance and repress gluconeogenic gene expression. Therefore, our study discovered a novel pathway to regulate the FOXO1-driven gluconeogenesis via DDB1-mediated CRY1 degradation.

RESEARCH DESIGN AND METHODS

Animals
Animal experiments were conducted in accordance with the guidelines of the institutional Animal Care and Use Committee of University of Michigan Medical School. Male *C57BL/6J* mice and *albumin-Cre* mice were purchased from The Jackson Laboratory. The *Ddb1^flox/flox^* mice were backcrossed to the *C57BL/6J* background for at least nine generations. The liver-specific *Ddb1* knockout (*Ddb1-LKO*) mice were generated by crossing *Ddb1^flox/flox^* mice with *albumin-Cre* mice. All mice were housed on a 12-h:12-h light:dark cycle at 25°C with free access to water and regular chow or HFD (45% kcal from fat; Research Diets). For fasting experiments, mice fasted for 16 h from 6:00 P.M. to 10:00 A.M.

Metabolic Parameter Measurements
Levels of blood glucose were measured with a Contour glucometer (Bayer). Aliquots of serum were analyzed for insulin levels by an insulin ELISA kit (R&D Systems). Pyruvate

tolerance tests (PTTs) were performed in fasting animals at the indicated time points after intraperitoneal injection of sodium pyruvate in saline at 2 g/kg.

RNA Isolation and Quantitative RT-PCR
The RNA isolation and quantitative RT-PCR (RT-qPCR) analysis were performed as previously described (28). The primer sequences used in qPCR analysis are listed in Supplementary Data. All gene expression experiments were performed in at least two independent experiments in biological triplicates.

Protein Extraction, Immunoprecipitation, and Ubiquitination Assay
For preparation of cytosolic and nuclear proteins, liver tissues or cell pellets were homogenized in hypotonic buffer, incubated on ice for 15–20 min, and centrifuged at 3,000 rpm for 10 min at 4°C. The supernatant was saved as cytosolic fraction. The pellet was washed once with hypotonic buffer and resuspended in radioimmunoprecipitation assay buffer prior to sonication for 5 s. The nuclear protein was then collected after centrifugation at 13,000 rpm × 10 min. Immunoprecipitation protocol to detect protein-protein interaction has previously been described (28). FLAG-M2 beads or streptavidin beads were added into the lysate to capture immunocomplex containing FLAG-CRY1 or CBP-CRY1. The protocol for detecting protein ubiquitination has previously been described (33). Anti-FOXO1 was used to pull down FOXO1-ubiquitin conjugates.

Proximity Ligation Assay
Proximity ligation assay (PLA) was performed using Duolink In Situ PLA reagent according to the instructions from Sigma-Aldrich. After overnight transduction with adenovirus expressing Foxo1 (Ad-Foxo1) and Ad-Cry1 in chamber slides, *Cry1^−/−^/Cry2^−/−^* mouse embryonic fibroblast (MEF) cells were fixed in 4% paraformaldehyde at 4°C for 10 min. After quenching with 0.1 mol/L glycine and permeabilization with 0.25% Triton-X 100, cells were blocked in 10% BSA and then incubated in 1:250 diluted primary antibody solutions (anti-FOXO1 H-128 [SC-11350] anti-CRY1 W-L5 [SC-101006]; Santa Cruz Biotechnology). Afterward, the slide was incubated in PLA mixture of Duolink In Situ Probe anti-Rabbit PLUS and Duolink In Situ Probe anti-Mouse MINUS in a preheated humidity chamber at 37°C for 1 h. After ligation and amplification at 37°C with Duolink In Situ Detection Reagents Far Red, the slide was mounted with coverslips using Duolink In Situ Mounting Medium with DAPI. Imaging was performed on a Zeiss Axio Imager M2 microscope with filters set at λEx = 360 nm/λEm = 460 nm for DAPI and at λEx = 647 nm/λEm = 669 nm for far red, where Ex is excitation and Em is emission. Nine individual fields under ×63 oil objective were captured for each condition and quantified using the ImageJ software.

Cell Cultures, Transfection, and Treatments
Both 293T and Hepa1c1c-7 cells were purchased from American Type Culture Collection and maintained according to the instructions. Transient transfection in 293T or

Hepa1 cells was performed using polyethylenimine (28). Primary mouse hepatocyte isolation has previously been described (28). Wild-type (WT) MEFs and *Cry1/2* double knockout MEF were generously provided by John Hogenesch (University of Cincinnati). Adenoviral transductions in cells were performed using 1.0×10^8 plaque-forming units per well of six-well plates for 16 h. For FOXO1 transcriptional activity assay, 293T cells in a 24-well plate were transfected with the *G6Pase*-luc construct (contains 1.2 kb promoter sequence upstream transcription starting site) alongside various combinations of expression vectors. Thirty-six hours posttransfection, cells were lysed for luciferase activity measurement on a Bio Tek Synergy 2 microplate reader. A β-galactosidase construct was cotransfected in each well for normalization of luciferase activity.

Generation and Injection of Recombinant Adenoviruses

Adenoviruses including Ad–short hairpin (sh)LacZ, Ad-shDdb1, Ad-Flag-Cry1-WT and Ad-Flag-Cry1–585KA, and Ad-Ddb1 have previously been described (28). Ad-FOXO1-ADA was generously provided by Henry Dong at the University of Pittsburg. Ad-Myc-Foxo1-WT was generated using previously described Gateway technology (28). Adeno-associated virus (AAV)-thyroxin binding globulin (TBG)-CRE and AAV-TBG-GFP were purchased from the University of Pennsylvania Vector Core. For adenoviral injections, 1×10^{12} plaque-forming units per adenovirus were administrated via tail vein injection. For each virus, a group of four to five mice were injected with the same dose of viral particles. Ten to fourteen days after injection, mice were sacrificed at Zeitgeber time (ZT) 8 after overnight fasting and liver tissues were harvested for protein analysis.

Western Blot

Western blot analysis was performed using the following primary antibodies: anti-DDB1 (Abcam), anti-CRY1 (sc-101006), anti-GAPDH (sc-25778), anti-Lamin A/C (sc-20681), anti-PEPCK (sc-32879), anti-G6PASE (sc-25840), anti-FOXO1 (sc-11350), anti-CUL4A (sc-10782), anti-AKT1/2 (sc-1619), anti-CBP (sc-33000) (Santa Cruz Biotechnology), anti–phosphorylated (phospho)-AKT (S473) and anti–phospho-glycogen synthase kinase (GSK)3β (S9) (Cell Signaling Technology), and anti-ubiquitin and anti–β-tubulin (Sigma-Aldrich). Anti-p85 was a gift from Liangyou Rui at the University of Michigan.

Statistical Analysis

All data are reported as mean $\pm$ SD. Differences between two groups were assessed by two-tailed Student t test. Difference between more than two groups was analyzed by ANOVA followed by Tukey post hoc testing. $P < 0.05$ was deemed statistically different.

RESULTS

Hepatocyte Deletion of *Ddb1* Impairs Glucose Metabolism in Regular Chow–Fed Mice

Thus far, the metabolic actions of DDB1 in the liver have never been tested. We set out to investigate whether *Ddb1* deficiency in hepatocytes could impact glucose metabolism in mice. We firstly confirmed *Ddb1* deletion in the *Ddb1-LKO* mouse liver and primary mouse hepatocytes by measuring DDB1 protein expression (Fig. 1A and Supplementary Fig. 1A). The residual DDB1 signal in *Ddb1-LKO* mouse liver was likely to be from other cell types within the liver, since the *Ddb1* mRNA is ubiquitously expressed (Supplementary Fig. 1B). In the same liver tissues, we observed increased levels of CRY1 protein (Fig. 1A), consistent with our previous report (28). Hepatocyte deletion of *Ddb1* reduced blood glucose levels during fasting and refeeding without affecting body weight (Fig. 1B–E), suggesting that DDB1 protein could act as a physiological regulator of glucose metabolism. The liver maintains steady levels of blood glucose during fasting by enhancing hepatic gluconeogenesis (34). For assessment of the role of DDB1 in this process, we performed pyruvate tolerance tests. Compared with $Ddb1^{flox/flox}$ mice, *Ddb1-LKO* mice showed impaired hepatic gluconeogenic response after gluconeogenic substrate pyruvate was injected (Fig. 1F). This reduction in gluconeogenic response is consistent with lowered protein and mRNA levels of PEPCK and G6Pase, two key enzymes in gluconeogenesis (Fig. 1G and H). These data, for the first time, demonstrated DDB1 as a new metabolic regulator of hepatic glucose metabolism.

Hepatocyte Deletion of *Ddb1* Protects Mice From HFD-Induced Hyperglycemia and Curbs Hepatic Gluconeogenesis

During the development of insulin resistance and type 2 diabetes caused by an HFD, unchecked gluconeogenesis in the liver is a major contributor to fasting hyperglycemia (35,36). Given the inhibitory effects of *Ddb1* deficiency on hepatic gluconeogenesis (Fig. 1F–H), we asked whether hepatic DDB1 level is affected by high-fat feeding. As shown in Fig. 2A, 12 weeks of HFD (45% calories from fat) markedly elevated the protein level of DDB1 in the mouse liver without affecting its binding partner CUL4A. This seems to be a liver-specific phenomenon, since DDB1 protein expression remained similar in adipose tissues from the same cohort of mice fed either regular chow or HFD (Fig. 2A). Moreover, induction of liver DDB1 protein by HFD possibly occurs through posttranslational modifications, since its mRNA levels are comparable between the regular chow and HFD groups (Supplementary Fig. 2A and B). Taken together, these studies suggest that the DDB1 protein abundance is sensitive to nutrient status in hepatocytes.

For testing of whether deletion of hepatic *Ddb1* could impact gluconeogenesis in mouse liver after HFD feeding, both $Ddb1^{flox/flox}$ and *Ddb1-LKO* mice were challenged with an HFD for 12 weeks. Compared with $Ddb1^{flox/flox}$ mice fed an HFD for 6–12 weeks, *Ddb1-LKO* mice displayed similar body weight gain (Fig. 2B) but lower levels of fasting glucose (Fig. 2C). Furthermore, *Ddb1-LKO* mice showed suppressed hepatic glucose production in PTTs after HFD feeding after 4 weeks of HFD feeding (Fig. 2D). Consistent with reduced glucose production in the liver, the mRNA and protein
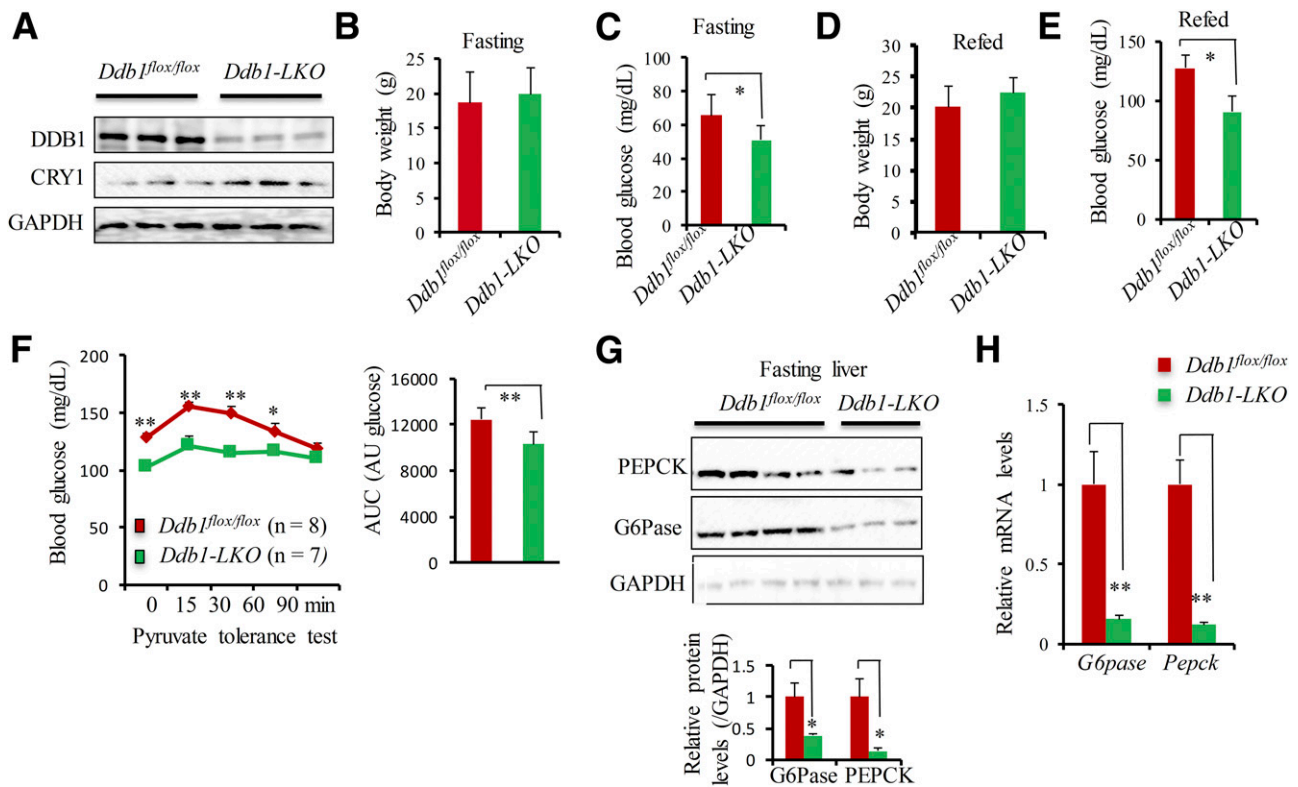
Figure 1—Loss of *Ddb1* in the liver impairs hepatic glucose metabolism in chow-fed mice. *Ddb1*$^{flox/flox}$ and *Ddb1-LKO* male mice (6–8 weeks) on regular chow feeding were compared in terms of body weight and blood glucose after either 12 h fasting or 8 h refeeding. *A*: Immunoblotting of DDB1 and CRY1 in the liver of *Ddb1*$^{flox/flox}$ and *Ddb1-LKO* mice (*n* = 3). *B* and *C*: Body weight and blood glucose in *Ddb1*$^{flox/flox}$ (*n* = 7) and *Ddb1-LKO* (*n* = 4) mice after 16 h fasting. *D* and *E*: Body weight and blood glucose in *Ddb1*$^{flox/flox}$ (*n* = 7) and *Ddb1-LKO* (*n* = 8) mice 8 h postrefeeding after 16 h fasting. *F*: PTT in *Ddb1*$^{flox/flox}$ (*n* = 8) and *Ddb1-LKO* (*n* = 6) mice after 16 h fasting. *G* and *H*: Protein and mRNA levels of *G6Pase* and *Pepck* in the liver of *Ddb1*$^{flox/flox}$ and *Ddb1-LKO* after 16 h fasting. Data were plotted as mean ± SD. *$P < 0.05$; **$P < 0.01$. AU, arbitrary units; AUC, area under the curve.

---

levels of G6Pase and PEPCK were reduced in *Ddb1-LKO* mice (Fig. 2*E* and *F*). Meanwhile, the nuclear CRY1 protein was enhanced in *Ddb1-LKO* mice (Fig. 2*F*). Taken together, our data suggested that hepatic *Ddb1* deficiency reduces blood glucose and suppresses hepatic gluconeogenesis during the course of an HFD. Of note, hepatic *Ddb1* deficiency shows no impact on systemic glucose utilization (measured by glucose tolerance test) and insulin sensitivity (by insulin tolerance test) after chronic HFD (Supplementary Fig. 3).

Acute Hepatocyte *Ddb1* Deficiency in Adult Mice Impairs HFD-Induced Hepatic Gluconeogenesis

To further test how hepatocyte DDB1 expression affects gluconeogenic response in adult mice, we used AAV-Cre to delete hepatic *Ddb1* in 8-week *Ddb1*$^{flox/flox}$ mice and then subjected them to HFD feeding for another 6 weeks (Fig. 3*A*). Acute *Ddb1* deletion did not affect body weight (Fig. 3*B*) but severely blunted hepatic gluconeogenesis response upon PTT (Fig. 3*C*). Even after 6 h of fasting we observed that mice injected with AAV-Cre showed higher blood glucose (134 mg/dL) in comparison with mice with AAV-GFP (77 mg/dL). Moreover, we detected significant reduction in *G6pase* and *Pepck* mRNA and protein expression in the liver

of HFD-treated AAV-Cre–injected *Ddb1*$^{flox/flox}$ mice (Fig. 3*D* and *E*). These data suggest that hepatic DDB1 in adult mice plays a crucial role in elevating hepatic glucose production in the context of HFD challenge.

Hepatic gluconeogenesis is mainly driven by transcription activators such as FOXO1, CREB, GR, and HNF-4α (2,3). It is possible that *Ddb1* deficiency could lead to impaired abilities of these transcription factors to promote gluconeogenesis. We focused on the potential role of FOXO1 because a recent study identified CRY1 as a suppressor of FOXO1 downstream of SREBP-1c (32). In a luciferase assay, *Ddb1* deficiency repressed the induction of the *G6pase* promoter–driven luciferase activity by Foxo1, whereas DDB1 overexpression augmented the luciferase activity (Supplementary Fig. 4). Although DDB1 functions as a scaffolding protein in the DDB1-CUL4A-CDT2 E3 ligase complex, we observed a great reduction in nuclear FOXO1 protein in *Ddb1*-deleted liver or hepatocytes (Fig. 3*F* and *G*). Moreover, inhibition of proteasomes by MG132 blocked the FOXO1 reduction caused by *Ddb1* depletion (Fig. 3*H*). These results suggest that DDB1 may control FOXO1 protein stability, and particularly nuclear FOXO1 abundance, to regulate gluconeogenic response.
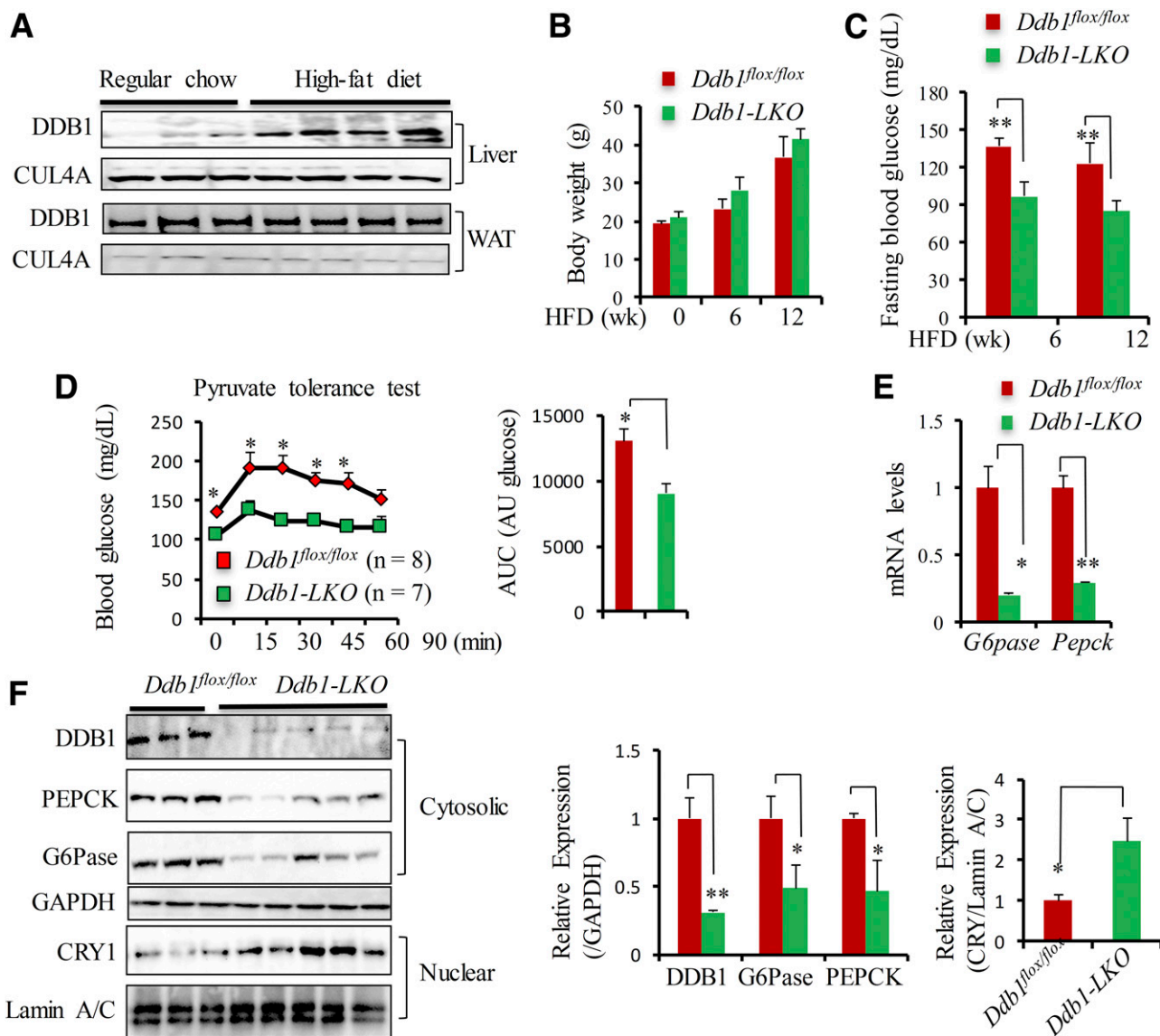
Figure 2—Hepatic deletion of *Ddb1* protects mice from HFD-induced hyperglycemia and gluconeogenesis. *A*: DDB1 and CUL4A protein in the liver and white adipose tissue of WT mice on regular chow vs. HFD feeding for 12 weeks. *B* and *C*: Body weight and fasting glucose of *Ddb1*flox/flox (*n* = 4) vs. *Ddb1-LKO* (*n* = 5) during 12 weeks of HFD. *D*: PTT after 4 weeks of HFD feeding in *Ddb1*flox/flox (*n* = 8) vs. *Ddb1-LKO* (*n* = 7) mice and area under the curve (AUC) analysis. *E*: The mRNA levels of *G6pase* and *Pepck* in the liver of *Ddb1*flox/flox (*n* = 8) vs. *Ddb1-LKO* (*n* = 7) after 12 weeks of HFD. *F*: Cytosolic levels of DDB1, CRY1, G6Pase, and PEPCK as well as nuclear CRY1 in the liver of *Ddb1*flox/flox vs. *Ddb1-LKO* mice after 12 weeks of HFD. Data are presented as mean ± SD. *P < 0.05; **P < 0.01. AU, arbitrary units; WAT, white adipose tissue; wk, weeks.

CRY1 Mediates the DDB1 Effects on FOXO1 Stabilization

Since DDB1 serves as a linker protein in the CUL4A ubiquitin E3 ligase complex, it is counterintuitive that *Ddb1* deficiency reduces FOXO1 protein abundance in our study. We speculated that this regulation could be mediated through one of the DDB1 substrates. We reported that the DDB1-CUL4A E3 ligase targets CRY1 for ubiquitination-dependent degradation to regulate the molecular clock activity and CRY1 level is increased in the *Ddb1*-deficient mouse liver (28). CRY1 has also been shown to be a negative regulator of hepatic gluconeogenesis mediated by GR, CREB, and,

most recently, FOXO1 (29,30,32). To test whether CRY1 protein might be a likely candidate to mediate FOXO1 degradation, we firstly compared the overall levels of the endogenous FOXO1 in WT versus $Cry1^{-/-}/Cry2^{-/-}$ MEF cells. Indeed, total FOXO1 protein expression is inversely correlated to total CRY1 protein (Fig. 4A). Next, we compared the nuclear abundance of FOXO1 protein in WT versus $Cry1^{-/-}/Cry2^{-/-}$ MEF cells, since it is the nuclear FOXO1 that drives the transcription of its target genes. The nuclear FOXO1 was also markedly increased in $Cry1^{-/-}/Cry2^{-/-}$ MEF (Fig. 4B). Conversely, restoring CRY1 expression in $Cry1^{-/-}/Cry2^{-/-}$ MEF was sufficient
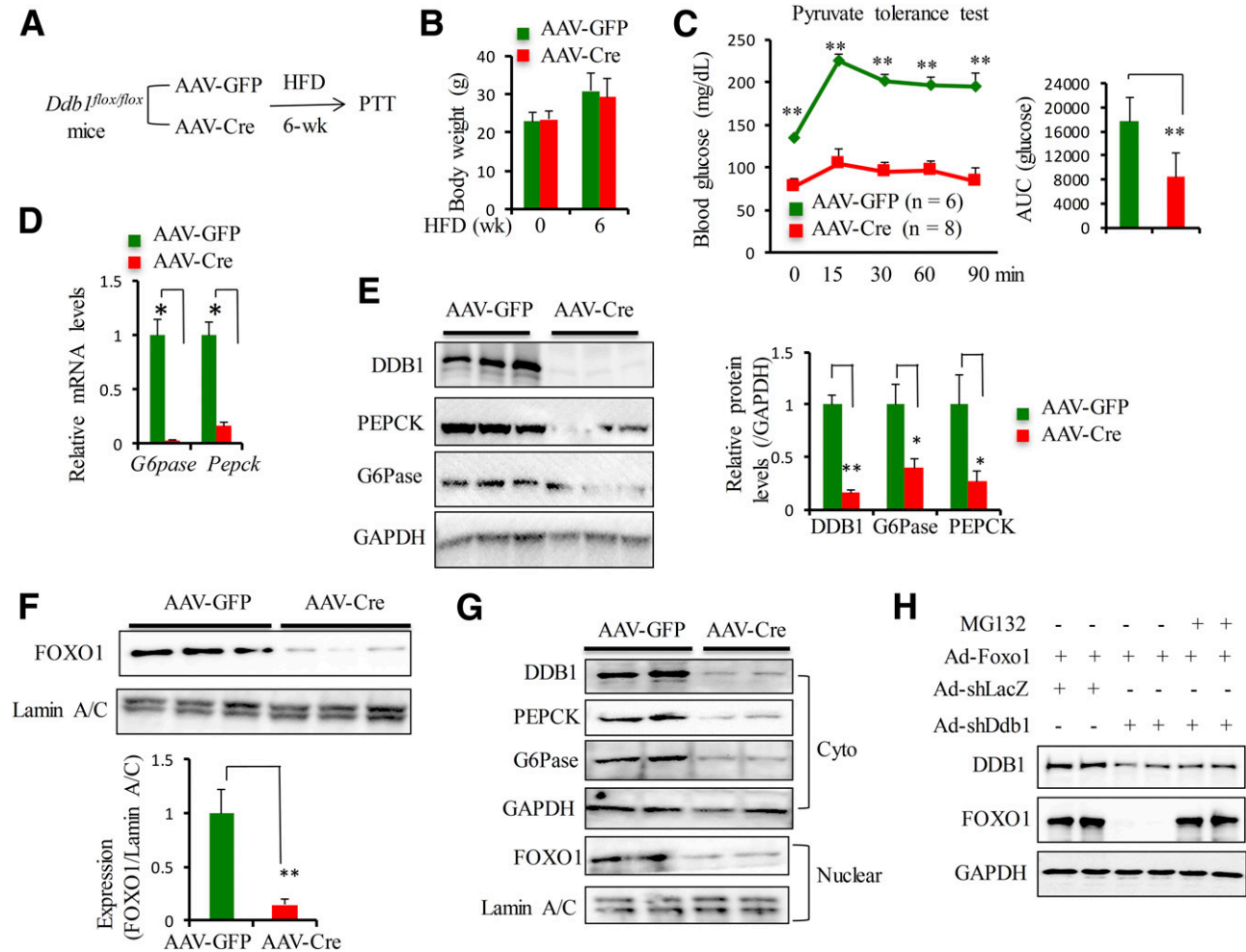
Figure 3—Acute adult-onset hepatic *Ddb1* deficiency impairs HFD-induced gluconeogenesis. *A*: Generation of acute adult-onset deletion of *Ddb1* in the liver by tail vein injection of *Ddb1^flox/flox* mice with AAV-TBG-Cre for PTT after 6 weeks of HFD. The control group mice were injected with AAV-TBG-GFP. *B*: Body weight of *Ddb1^flox/flox* mice injected with either AAV-GFP ($n = 6$) or AAV-Cre ($n = 8$) before and after HFD. *C*: PTT after 6 weeks of HFD in AAV-GFP vs. AAV-Cre group mice and area under the curve (AUC) analysis. *D*: The mRNA levels of *G6pase* and *Pepck* in the liver of AAV-GFP vs. AAV-Cre group mice after 7 weeks of HFD. *E* and *F*: Cytosolic levels of DDB1, G6Pase, and PEPCK and nuclear FOXO1 protein in the liver of AAV-GFP vs. AAV-Cre group mice after 7 weeks of HFD. *G*: Nuclear FOXO1 protein in the *Ddb1^flox/flox* PMHs transduced with AAV-GFP vs. AAV-Cre. Cytosolic (Cyto) levels of DDB1, G6Pase, and PEPCK were also examined by immunoblotting. *H*: Rescue of FOXO1 protein expression by proteasome inhibitor MG132 in Ad-shDdb1–transduced Hepa1 cells. Hepa1 cells were first transduced with Ad-Foxo1 in addition to either Ad-shLacZ or Ad-shDdb1. Forty-eight hours later, cells were treated with MG132 (10 μmol/L) for 8 h before harvest or were not treated. Protein levels of DDB1, FOXO1, and GAPDH were examined by immunoblotting. *$P < 0.05$; **$P < 0.01$. wk, weeks.

to reduce the nuclear FOXO1 abundance (Fig. 4*B*). It is known that nuclear FOXO1 abundance is influenced by either stability and/or localization. To distinguish these possibilities, we performed a similar experiment using the mutant FOXO1 (FOXO1-ADA) that is constitutively localized in the nucleus owing to the loss of AKT-dependent phosphorylation (7). Similar to FOXO1-WT, the levels of FOXO1-ADA were also increased in the *Cry1^−/−/Cry2^−/−* MEF (Fig. 4*C*). Taken together, our data suggest that CRY1 downregulates mainly the nuclear FOXO1 protein abundance.

To directly address whether CRY1 could be a downstream mediator linking DDB1 and FOXO1, we performed acute knockdown of *Ddb1* in Ad-Foxo1–transduced WT and *Cry1^−/−/Cry2^−/−* MEF cells. In agreement with

AAV-Cre–transduced *Ddb1^flox/flox* mouse liver and primary mouse hepatocytes (PMHs) (Fig. 3*F* and *G*), *Ddb1* depletion reduced the nuclear FOXO1 protein in WT MEF but not in *Cry1^−/−/Cry2^−/−* MEF (Fig. 4*D*). Conversely, overexpression of DDB1 increased nuclear FOXO1 in WT MEF but not in *Cry1^−/−/Cry2^−/−* MEF (Fig. 4*E*). These data support that DDB1 promotes the nuclear FOXO1 abundance via degrading CRY1.

CRY1 Interacts With FOXO1 and Promotes Its Ubiquitination and Degradation

To further explore how CRY1 regulates FOXO1 protein turnover, we measured levels of poly-ubiquitinated FOXO1 protein in WT or *Cry1^−/−/Cry2^−/−* MEF cells by
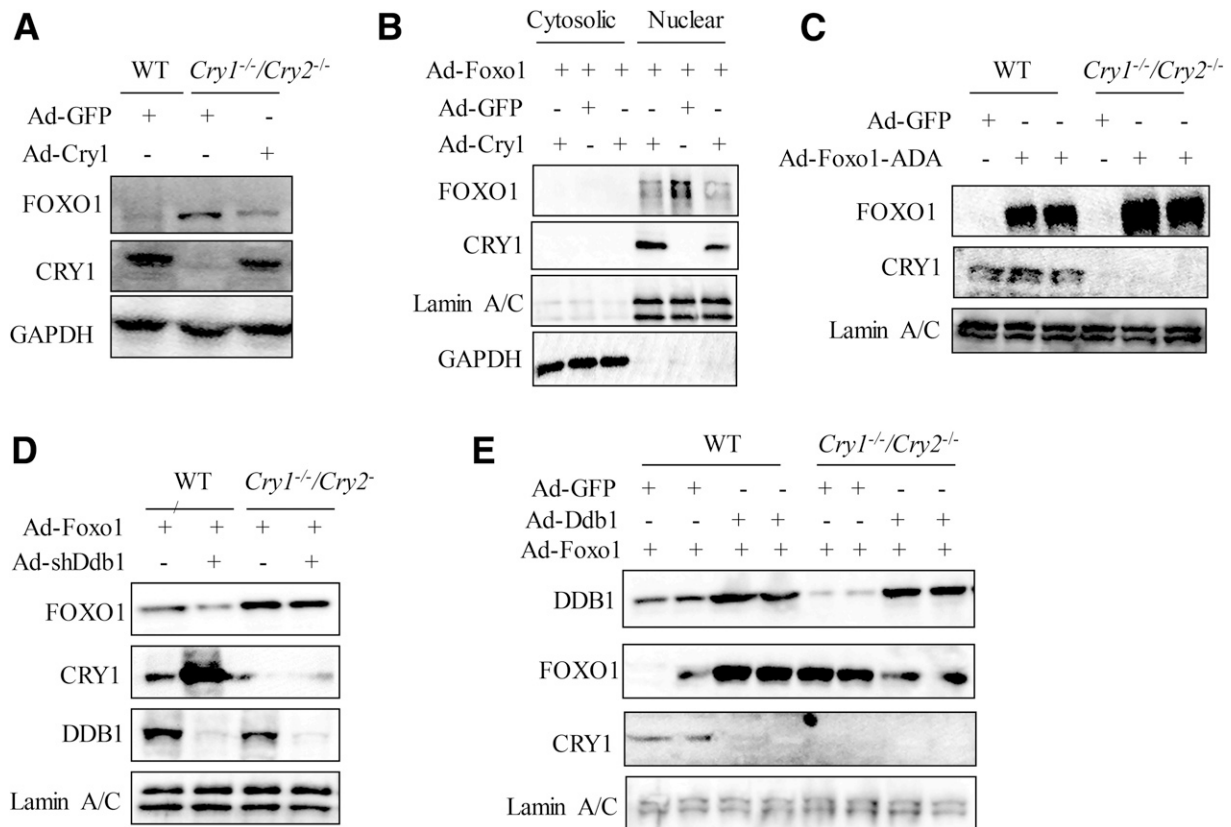
A

B

C

D

E

Figure 4—DDB1 represses FOXO1 through CRY1. *A*: Levels of total FOXO1 protein in the WT and *Cry1*$^{-/-}$/*Cry2*$^{-/-}$ MEF cells transduced with Ad-Cry1. Cells were harvested 36 h post–adenoviral transduction. *B*: Restoring CRY1 expression reduces nuclear FOXO1 protein in *Cry1*$^{-/-}$/*Cry2*$^{-/-}$ MEF cells. WT and *Cry1*$^{-/-}$/*Cry2*$^{-/-}$ MEF cells were transduced with Ad-Foxo1 plus either Ad-GFP or Ad-Cry1. Thirty-six hours posttransduction, FOXO1 protein in the nuclear extracts was detected by Western blot. *C*: Accumulation of FOXO1-ADA protein in the *Cry1*$^{-/-}$/*Cry2*$^{-/-}$ MEF. WT vs. *Cry1*$^{-/-}$/*Cry2*$^{-/-}$ MEFs transduced with Ad-Foxo1-ADA. Thirty-six hours posttransduction, FOXO1-ADA protein in the nuclear extracts was detected by Western blot. *D*: Acute *Ddb1* depletion reduces the nuclear abundance of FOXO1 protein in WT MEF but not *Cry1*$^{-/-}$/*Cry2*$^{-/-}$ MEF cells. Both WT and *Cry1*$^{-/-}$/*Cry2*$^{-/-}$ MEF cells were first transduced with Ad-shLacZ or Ad-shDdb1 for 6 h prior to transduction with Ad-Foxo1. Nuclear FOXO1 protein was detected by Western blot 36 h posttransduction. *E*: Effects of DDB1 overexpression on nuclear FOXO1 in WT and *Cry1*$^{-/-}$/*Cry2*$^{-/-}$ MEF cells. Both WT and *Cry1*$^{-/-}$/*Cry2*$^{-/-}$ MEF cells were first transduced with Ad-GFP or Ad-Ddb1 6 h prior to transduction with Ad-Foxo1. Nuclear FOXO1 protein was detected by Western blot 36 h posttransduction.

immunoblotting with anti-ubiquitin after immunoprecipitation (IP) with anti-FOXO1. Ubiquitination of FOXO1 was greatly reduced in *Cry1*$^{-/-}$/*Cry2*$^{-/-}$ MEF (Fig. 5*A*). In contrast, *Cry1* overexpression enhanced the formation of polyubiquitinated FOXO1 in WT MEF cells (Fig. 5*B*). These data suggest that CRY1 downregulates FOXO1 protein stability by promoting its ubiquitination and degradation.

How does CRY1 promote FOXO1 ubiquitination and degradation? It is possible that CRY1 could interact with FOXO1 and recruit its E3 ligase. Indeed, a strong interaction of CRY1 was detected with either FOXO1-WT or FOXO1-ADA in cotransfected 293T cells and transduced PMHs (Fig. 5*C–E*). The protein interaction between CRY1 and FOXO1 in the nucleus was further validated by a proximity ligation assay with anti-FOXO1 and anti-CRY1 in *Cry1*$^{-/-}$/*Cry2*$^{-/-}$ MEF cells transduced with both Ad-Cry1 and Ad-Foxo1 (Fig. 5*F*). Furthermore, such interaction was found to require the CRY1-terminal region (300–614 aa) after domain mapping via a series of CRY1 truncation mutants (Supplementary Fig. 6).

Cry1 Depletion Abrogates Insulin-Induced Suppression of FOXO1 Activity

Upon food intake, insulin suppresses FOXO1 transcription via insulin receptor (InsR)-AKT signaling (5,7). Whether CRY1 contributes to insulin-induced suppression of FOXO1 action has not been tested yet. We observed that CRY1 protein in primary hepatocytes was quickly induced within 1 h of treatment with insulin (Fig. 6*A*). Such regulation was also observed in the fasted mouse livers 2 h after insulin injection (Fig. 6*B*). In both cases, the *Cry1* mRNA remained unchanged (Supplementary Fig. 7) within 2 h of insulin treatment, suggesting that insulin is likely to promote CRY1 protein stabilization independently of transcriptional activation during the first 2 h of insulin exposure.

Next, we asked whether CRY1 could affect insulin-induced nuclear FOXO1 protein degradation in mouse hepatocytes (15,16). Consistent with the literature (6,7), insulin treatment reduces the nuclear FOXO1 in Ad-shLacZ–transduced PMHs. However, its effect was abolished in the
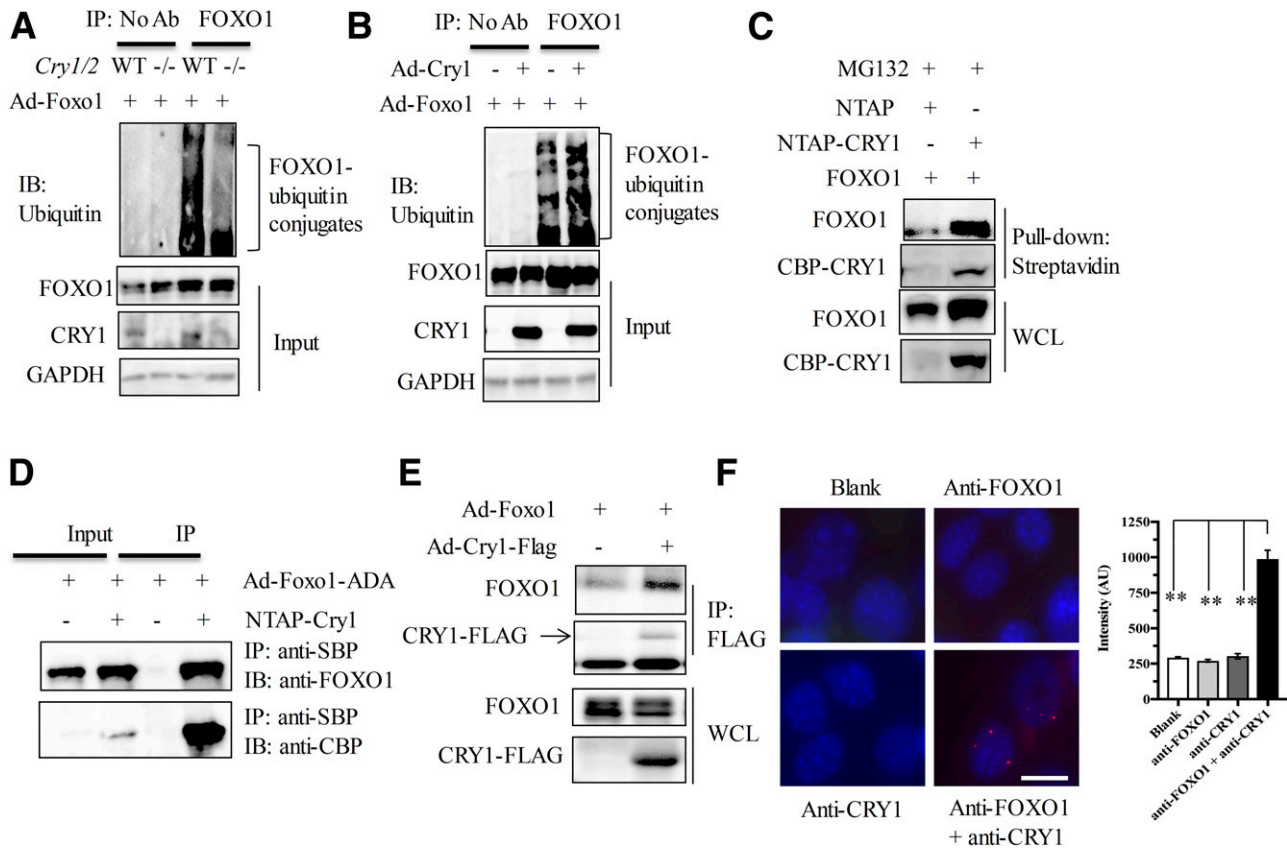
Figure 5—CRY1 interacts with FOXO1 and promotes its ubiquitination. *A*: Reduced FOXO1 ubiquitination in Cry1/2-null MEF cells. Both WT and *Cry1⁻/⁻/Cry2⁻/⁻* MEF were transduced with Ad-FOXO1 and treated with MG132 for 4 h. The denatured cell lysates were subjected to IP with anti-FOXO1 and then immunoblotting (IB) with anti-ubiquitin. *B*: CRY1 overexpression increases FOXO1 ubiquitination in *Cry1⁻/⁻/Cry2⁻/⁻* MEF cells. *Cry1⁻/⁻/Cry2⁻/⁻* MEF cells were transduced with Ad-GFP vs. Ad-Cry1 for 6 h and transduced again with Ad-Foxo1. After treatment with MG132 for 4 h, the denatured cell lysates were subjected to IP with anti-FOXO1 and then immunoblotting with anti-ubiquitin to examine FOXO1 ubiquitination. *C* and *D*: CRY1 interacts with FOXO1 WT or FOXO1-ADA in 293T cells. 293T cells were cotransfected with Foxo1 plus NTAP alone or NTAP-Cry1. After pull-down with streptavidin beads, the CRY complex was subjected to immunoblotting with anti-FOXO1 and anti-CBP. *E*: CRY1 interacts with FOXO1 in PMHs. After transduction with Ad-Foxo1 plus Ad-GFP or Ad-Cry1, PMHs were subjected to IP with anti-FLAG and Western blot for FOXO1 and FLAG-CRY1. *F*: CRY1 interaction with FOXO1 in the nucleus by PLA. After transduction with Ad-Foxo1 and Ad-Cry1, *Cry1⁻/⁻/Cry2⁻/⁻* MEF cells were incubated with both anti-CRY1 and anti-FOXO1 antibodies and subjected to PLA with Duolink In Situ PLA probes. No antibody and single-antibody incubation were included as negative controls. Scale bar = 20 μm. Data are presented as mean ± SD. **$P < 0.01$. Ab, antibody; AU, arbitrary units; WCL, whole cell lysate.

Ad-shCry1–transduced PMHs (Fig. 6*C*), suggesting that CRY1 is required for insulin-induced nuclear FOXO1 degradation. To further test the role of CRY1 in insulin suppression of gluconeogenesis, we compared the mRNA levels of *G6Pase* and *Pepck* in PMHs transduced with Ad-shCry1 versus Ad-shLacZ. As shown in Fig. 6*D* and *E*, insulin potently suppresses mRNA of *G6Pase* and *Pepck* in a dose-dependent manner in cells transduced with Ad-shLacZ but not in cells transduced with Ad-shCry1. Intriguingly, *Pepck* mRNA was significantly increased in cells transduced with Ad-shCry1 after insulin treatment. Thus, CRY1 is required for insulin-induced suppression of nuclear FOXO1 and gluconeogenic gene expression in hepatocytes.

Acute Depletion of *Cry1* in Mice Leads to Elevated Fasting Glucose and Gluconeogenic Response

To further evaluate the impact of *Cry1* depletion on glucose metabolism in vivo, we injected WT mice with Ad-shCry1 versus Ad-shLacZ via tail vein. The CRY1 protein was measured in the mouse liver 14 days postinjection. CRY1 protein levels were reduced in Ad-shCry1–injected liver, whereas FOXO1 protein was elevated (Fig. 7*A*). Seven days after injection, we detected a significant increase in blood glucose level in Ad-shCry1–injected mice after overnight fasting compared with Ad-shLacZ–injected mice (Fig. 7*B*), a phenotype similar to that in *Cry1* and *Cry2* double knockout mice (29,37). To assess the gluconeogenic activity in the *Cry1*-depleted liver, we performed PTTs in both groups of mice at 7 days postinjection. Consistently, we observed a significant increase in blood glucose in response to pyruvate in mice injected with Ad-shCry1 (Fig. 7*C*). The serum insulin levels were slightly reduced in the shCry1 group without statistical significance (Fig. 7*D*). Meanwhile, the levels of *G6Pase*, *Pepck*, and *Pgc-1α* (coactivator for gluconeogenesis) were significantly induced (Fig. 7*E*). Taken together, our data support CRY1 as a negative regulator of hepatic gluconeogenesis in vivo.
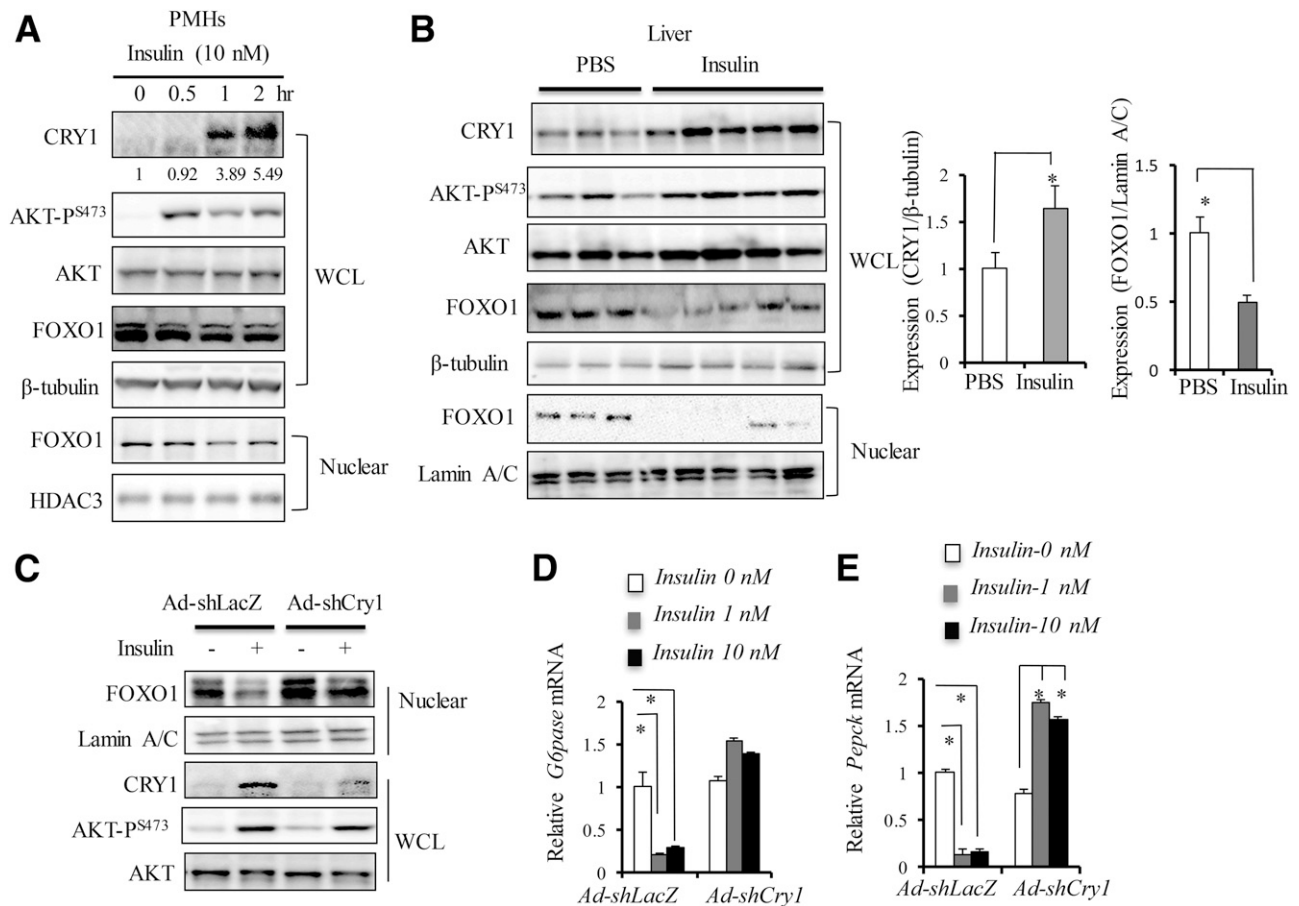
Figure 6—CRY1 is required for insulin-induced suppression of gluconeogenesis. A: Insulin increases CRY1 protein levels in primary mouse hepatocytes. The endogenous CRY1 protein in PMHs was detected by Western blot after insulin treatment at 10 nmol/L for the indicated durations. The number refers to the fold induction of CRY1 protein after normalization to the level of β-tubulin. Both total FOXO1 and nuclear FOXO1 protein levels were measured as well. B: Insulin increases CRY1 protein levels but reduces nuclear FOXO1 protein in the mouse liver. WT mice were fasted for 6 h prior to intraperitoneal injection of insulin at 1 units/kg for 2 h. Hepatic CRY1 was detected by Western blot and its fold of induction by insulin was calculated after normalization to β-tubulin. Both total FOXO1 and nuclear FOXO1 protein levels were measured as well. C: Depletion of *Cry1* impairs insulin action on nuclear FOXO1 protein. PMHs were transduced with Ad-shLacZ or Ad-shCry1 for 24 h and transduced by Ad-Foxo1 for an additional 24 h. PMHs were serum starved for 16 h and then stimulated with insulin at 10 nmol/L for 2 h. Nuclear abundance of FOXO1 and CRY1 was examined by immunoblotting. D and E: *Cry1* knockdown abrogates insulin actions on the *G6pase* and *Pepck* expression. PMHs were transduced with Ad-shLacZ or Ad-shCry1 for 24 h and serum starved overnight prior to insulin treatment and RT-qPCR analysis. Data are presented as mean ± SD. *$P < 0.05$. hr, hours; WCL, whole cell lysate.

Cry1 and *Cry2* double knockout mice develop systemic insulin resistance when challenged with HFD (37). However, the tissue-specific role of CRY1 in insulin sensitivity remains unclear. To gain insights into the impact of chronic *Cry1* depletion on liver insulin signaling, we examined the phosphorylation levels of downstream targets of insulin in the Ad-shCry1–injected liver after 2 weeks of HFD feeding. Consistent with elevated gluconeogenesis, the levels of AKT-P^{S473} and GSK3β-P^{S9} were reduced in the liver with acute *Cry1* knockdown in HFD-fed mice (Fig. 7F), suggesting that chronic *Cry1* depletion could lead to impairment of insulin-AKT signaling, which further promotes FOXO1 accumulation in the liver. To confirm that this indeed occurs in hepatocytes, we isolated PMH from mice injected with shCry1 for >7 days and found that these hepatocytes were also very resistant to insulin-stimulated AKT-P^{S473} (Supplementary Fig. 8).

To gain insights into how chronic *Cry1* deficiency may lead to insulin resistance in hepatocytes, we performed RT-qPCR analysis of known genes associated with insulin resistance either in mice injected with Ad-shLacZ or in mice after HFD feeding. In both liver and PMHs of Ad-shCry1–injected mice, the expression of the known negative regulator of insulin signaling *Socs3* was significantly increased (Supplementary Fig. 9A and B) (38,39). Induction of *Dbp* mRNA was used as a marker for *Cry1* depletion. Since CRY1 has been also implicated in inhibiting inflammation in various tissues (40,41) and chronic inflammation has been linked to insulin resistance (42,43), we checked the expression of several proinflammatory markers in the liver of Ad-shCry1–injected mice. As shown in Supplementary Fig. 9C, hepatic *Cry1* depletion increased the expression of *Tnfα* and *Mcp-1* in the liver of Ad-shCry1–injected mice. Taken together, our data showed that acute *Cry1* deficiency results
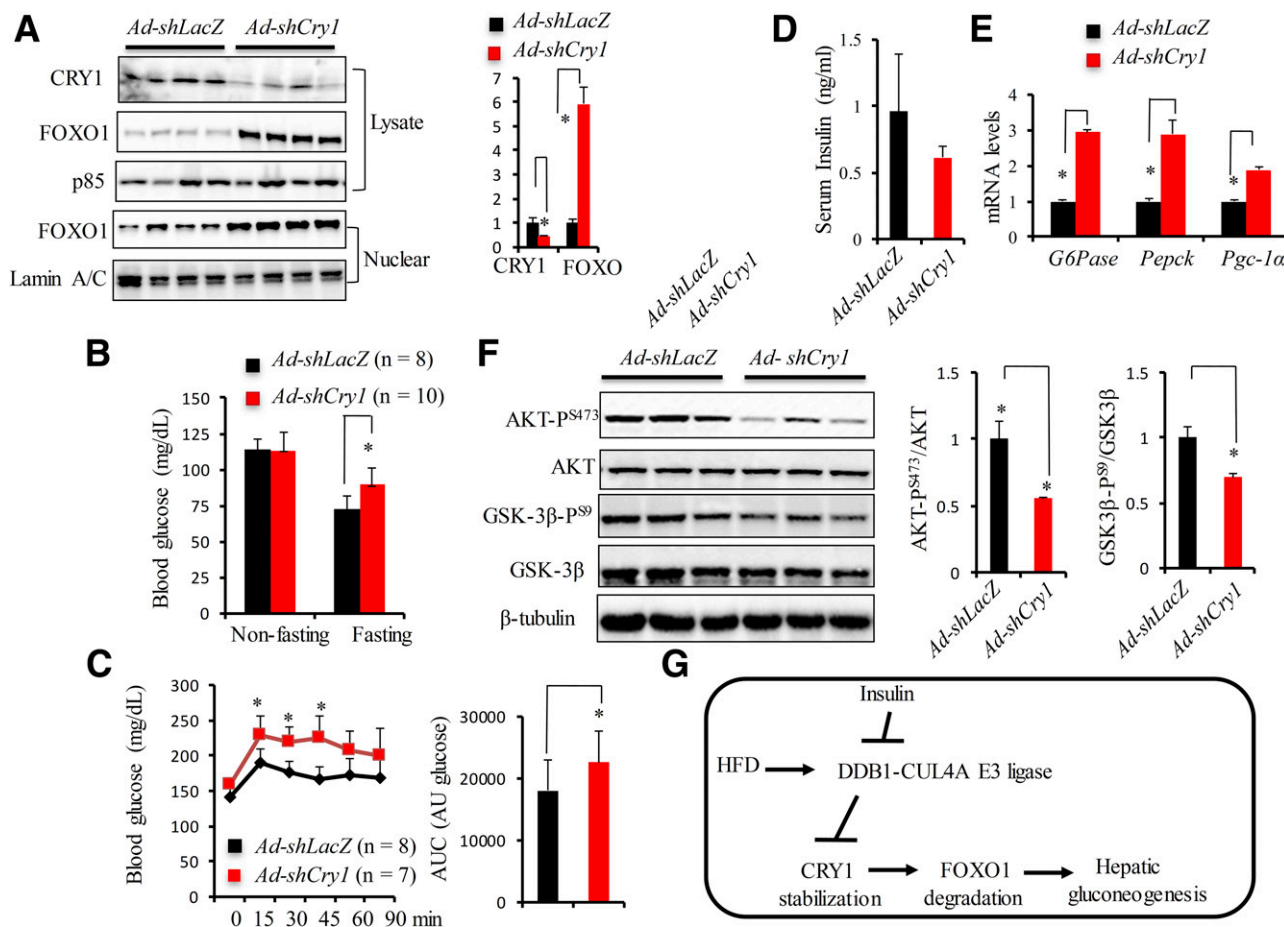
Figure 7—Chronic depletion of CRY1 promotes hepatic gluconeogenesis. WT mice were injected with Ad-shLacZ vs. Ad-shCry1 via tail vein and examined as follows. *A*: Levels of CRY1 and FOXO1 protein in the liver by Western blot 14 days after injection. Nuclear FOXO1 protein in the same liver tissues was also detected and quantified by immunoblotting. *B*: Nonfasting and fasting blood glucose levels 10 days after injection. *C*: PTT 7 days after injection. *D*: Serum levels of insulin after 6 h fasting 14 days after injection. *E*: RT-qPCR analysis for the mRNA expression of *G6pase*, *Pepck*, and *Pgc-1α* in the liver 14 days after injection. *F*: AKT and GSK3β phosphorylation levels in the liver 14 days after injection. The ratios of AKT-P^{S473} to AKT and GSK3β-P to GSK3β were calculated. *G*: The schematics of DDB1 regulation of hepatic gluconeogenesis through CRY1. In the absence of insulin, DDB1-CUL4A-CDT2 E3 ligase ubiquitinates CRY1 for proteasomal degradation. Decreased CRY1 leads to stabilization of FOXO1 and thus promotes gluconeogenesis. In *Ddb1*-deficient hepatocytes, CRY1 stabilization results in constant degradation of FOXO1 and reduced gluconeogenesis. Data are presented as mean ± SD. *$P < 0.05$. AU, arbitrary units; AUC, area under the curve.

in hepatic insulin resistance by upregulating the pathways that impede insulin signaling and subsequently exacerbate the FOXO1-driven gluconeogenesis.

DISCUSSION

Uncontrolled hepatic glucose production is a hallmark of type 2 diabetes (2,35). Here, we uncovered a novel metabolic pathway in which DDB1 E3 ligase promotes FOXO1-driven hepatic gluconeogenesis by degrading CRY1. Furthermore, deletion of *Ddb1* in hepatocytes protects mice from HFD-induced fasting hyperglycemia and elevated gluconeogenesis without affecting body weight. In addition, we demonstrated that insulin induces CRY1 protein and CRY1 depletion impairs insulin's ability to suppress FOXO1-mediated gluconeogenesis. In conclusion, our study discovered DDB1-mediated CRY1 degradation as a novel pathway to regulate FOXO1 protein expression and gluconeogenesis in the liver

(Fig. 7G). Given that a specific small-molecule activator of CRY1 has been shown to repress glucagon-induced gluconeogenesis in PMHs (44), suppression of DDB1 E3 ligase–mediated ubiquitination and degradation of CRY1 may offer another therapeutic avenue to control hyperglycemia in people with type 2 diabetes.

Targeted protein ubiquitination and degradation have been shown to regulate cell cycle, genomic stability, and DNA replication (45,46). How protein ubiquitination regulates metabolic events is far less understood. Emerging evidence suggests that E3 ligases could be important regulators of glucose metabolism (47). For example, the ubiquitin E3 ligase MG53 promotes IRS-1 ubiquitination and degradation and therefore contributes to obesity and metabolic syndrome upon chronic HFD (48,49). In contrast, the ubiquitin E3 ligase CBL-B promotes ubiquitination and degradation of TLR4 and therefore reduces macrophage activation

and infiltration during obesity (50). Collectively, these findings suggest that E3 ligases could be effectively targeted to restore metabolic homeostasis. In our current study, we provide both in vivo and in vitro evidence suggesting an important role of DDB1-CUL4A E3 ligase in hepatic glucose metabolism. *Ddb1* deficiency represses FOXO1-driven gluconeogenesis in hepatocytes and in turn reduces blood glucose during fasting. Interestingly, DDB1 protein is elevated in the mouse liver after HFD, raising the possibility that induction of DDB1 might be required to protect FOXO1 stability during insulin resistance. Since CRY1 has also been implicated to suppress the cAMP-CREB and glucocorticoid-mediated gluconeogenesis pathway (29,30), it remains to be tested whether DDB1 could also regulate these two pathways in addition to FOXO1 in both fasting and HFD conditions.

We provide the first evidence that insulin induces CRY1 protein expression independently of gene expression in both hepatocytes and liver. We propose two possible mechanisms that may account for such an acute action of insulin on CRY1 stability. The first possibility is that the insulin-AKT signaling pathway promotes phosphorylation of CRY1 to block its interaction with DDB1-CUL4A-CDT2 E3 ligase, therefore protecting CRY1 from degradation. However, sequence analysis by Scansite revealed that CRY1 contains no canonical phosphorylation motifs for AKT. The second possibility is that insulin can block the formation of DDB1-CUL4A-CDT2 E3 ligase. Two recent reports highlighted a role of FBOX11 E3 ligase in promoting CDT2 ubiquitination and degradation in response to TGF-β signaling (51,52), implying a possibility of signal-dependent CDT2 protein degradation. Sequence analysis suggests that CDT2 is a preferred substrate for a number of kinases including AKT, GSK3β, ATM, and DNA-dependent protein kinase. Thus, CDT2 could be a potential direct target of AKT to modulate DDB1-CUL4A E3 ligase activity. More detailed biochemical analysis will be needed to determine whether insulin inhibits DDB1-CUL4A-CDT2 E3 ligase assembly and activity via direct phosphorylation.

Unexpectedly, we observed that acute Cry1 deficiency leads to a marked reduction in AKT activation in both liver and primary mouse hepatocytes. This effect might be due to a combination of induction of both negative regulator of insulin signaling (SOCS3) and proinflammatory markers. How CRY1 is involved in suppressing these pathways remains to be addressed. These findings also suggest that CRY1 can inhibit FOXO1 signaling via two distinctive mechanisms in a time-dependent manner: on one hand, CRY1 acutely binds to nuclear FOXO to promote its ubiquitination-dependent degradation. On the other hand, chronic activation of CRY1 could enhance AKT signaling and therefore facilitates the translocation of FOXO1 to the nucleus to further inhibit gluconeogenic gene expression.

In conclusion, our study has identified an intricate mechanism of how DDB1 stabilizes FOXO1 through CRY1 degradation during fasting. Our study highlighted the critical role of DDB1 in promoting FOXO-1–dependent gluconeogenesis in the liver. Given the function of DDB1 in the CUL4A E3 ligase complex, it is conceivable that targeting DDB1 might offer novel therapeutics for the treatment of type 2 diabetes.

Author Contributions. X.T. and L.Y. designed and performed in vitro experiments. X.T. and L.Y. wrote and edited the manuscript. X.T., D.Z., N.C., and K.V. conducted in vivo experiments. E.J., K.S., and N.G. carried out RT-qPCR and the generation of adenoviral constructs and concentration of adenoviruses. J.S. analyzed and quantified the PLA imaging data. L.Y. supervised the work and analyzed and interpreted data. L.Y. is the guarantor of this work and, as such, had full access to all the data in the study and takes responsibility for the integrity of the data and the accuracy of the data analysis.

References

1. Biddinger SB, Kahn CR. From mice to men: insights into the insulin resistance syndromes. Annu Rev Physiol 2006;68:123–158
2. Lin HV, Accili D. Hormonal regulation of hepatic glucose production in health and disease. Cell Metab 2011;14:9–19
3. Pilkis SJ, Granner DK. Molecular physiology of the regulation of hepatic gluconeogenesis and glycolysis. Annu Rev Physiol 1992;54:885–909
4. Michael MD, Kulkarni RN, Postic C, et al. Loss of insulin signaling in hepatocytes leads to severe insulin resistance and progressive hepatic dysfunction. Mol Cell 2000;6:87–97
5. Accili D, Arden KC. FoxOs at the crossroads of cellular metabolism, differentiation, and transformation. Cell 2004;117:421–426
6. Barthel A, Schmoll D, Unterman TG. FoxO proteins in insulin action and metabolism. Trends Endocrinol Metab 2005;16:183–189
7. Brunet A, Bonni A, Zigmond MJ, et al. Akt promotes cell survival by phosphorylating and inhibiting a Forkhead transcription factor. Cell 1999;96:857–868
8. Nakae J, Kitamura T, Ogawa W, Kasuga M, Accili D. Insulin regulation of gene expression through the forkhead transcription factor Foxo1 (Fkhr) requires kinases distinct from Akt. Biochemistry 2001;40:11768–11776
9. Nakae J, Kitamura T, Silver DL, Accili D. The forkhead transcription factor Foxo1 (Fkhr) confers insulin sensitivity onto glucose-6-phosphatase expression. J Clin Invest 2001;108:1359–1367
10. Nakae J, Park BC, Accili D. Insulin stimulates phosphorylation of the forkhead transcription factor FKHR on serine 253 through a Wortmannin-sensitive pathway. J Biol Chem 1999;274:15982–15985
11. Puigserver P, Rhee J, Donovan J, et al. Insulin-regulated hepatic gluconeogenesis through FOXO1-PGC-1alpha interaction. Nature 2003;423:550–555
12. Lu M, Wan M, Leavens KF, et al. Insulin regulates liver metabolism in vivo in the absence of hepatic Akt and Foxo1. Nat Med 2012;18:388–395
13. Matsumoto M, Pocai A, Rossetti L, Depinho RA, Accili D. Impaired regulation of hepatic glucose production in mice lacking the forkhead transcription factor Foxo1 in liver. Cell Metab 2007;6:208–216
14. Huang H, Tindall DJ. Regulation of FOXO protein stability via ubiquitination and proteasome degradation. Biochim Biophys Acta 2011;1813:1961–1964

15. Matsuzaki H, Daitoku H, Hatta M, Tanaka K, Fukamizu A. Insulin-induced phosphorylation of FKHR (Foxo1) targets to proteasomal degradation. Proc Natl Acad Sci U S A 2003;100:11285–11290

16. Plas DR, Thompson CB. Akt activation promotes degradation of tuberin and FOXO3a via the proteasome. J Biol Chem 2003;278:12361–12366

17. Fu W, Ma Q, Chen L, et al. MDM2 acts downstream of p53 as an E3 ligase to promote FOXO ubiquitination and degradation. J Biol Chem 2009;284:13987–14000

18. Huang H, Regan KM, Wang F, et al. Skp2 inhibits FOXO1 in tumor suppression through ubiquitin-mediated degradation. Proc Natl Acad Sci U S A 2005;102:1649–1654

19. Kato S, Ding J, Pisck E, Jhala US, Du K. COP1 functions as a FoxO1 ubiquitin E3 ligase to regulate FoxO1-mediated gene expression. J Biol Chem 2008;283:35464–35473

20. Angers S, Li T, Yi X, MacCoss MJ, Moon RT, Zheng N. Molecular architecture and assembly of the DDB1-CUL4A ubiquitin ligase machinery. Nature 2006;443:590–593

21. He YJ, McCall CM, Hu J, Zeng Y, Xiong Y. DDB1 functions as a linker to recruit receptor WD40 proteins to CUL4-ROC1 ubiquitin ligases. Genes Dev 2006;20:2949–2954

22. Iovine B, Iannella ML, Bevilacqua MA. Damage-specific DNA binding protein 1 (DDB1): a protein with a wide range of functions. Int J Biochem Cell Biol 2011;43:1664–1667

23. Jin J, Arias EE, Chen J, Harper JW, Walter JC. A family of diverse Cul4-Ddb1-interacting proteins includes Cdt2, which is required for S phase destruction of the replication factor Cdt1. Mol Cell 2006;23:709–721

24. Cang Y, Zhang J, Nicholas SA, et al. Deletion of DDB1 in mouse brain and lens leads to p53-dependent elimination of proliferating cells. Cell 2006;127:929–940

25. Cang Y, Zhang J, Nicholas SA, Kim AL, Zhou P, Goff SP. DDB1 is essential for genomic stability in developing epidermis. Proc Natl Acad Sci U S A 2007;104:2733–2737

26. Li B, Jia N, Kapur R, Chun KT. Cul4A targets p27 for degradation and regulates proliferation, cell cycle exit, and differentiation during erythropoiesis. Blood 2006;107:4291–4299

27. Wertz IE, O'Rourke KM, Zhang Z, et al. Human De-etiolated-1 regulates c-Jun by assembling a CUL4A ubiquitin ligase. Science 2004;303:1371–1374

28. Tong X, Zhang D, Guha A, et al. CUL4-DDB1-CDT2 E3 ligase regulates the molecular clock activity by promoting ubiquitination-dependent degradation of the mammalian CRY1. PLoS One 2015;10:e0139725

29. Lamia KA, Papp SJ, Yu RT, et al. Cryptochromes mediate rhythmic repression of the glucocorticoid receptor. Nature 2011;480:552–556

30. Zhang EE, Liu Y, Dentin R, et al. Cryptochrome mediates circadian regulation of cAMP signaling and hepatic gluconeogenesis. Nat Med 2010;16:1152–1156

31. Kume K, Zylka MJ, Sriram S, et al. mCRY1 and mCRY2 are essential components of the negative limb of the circadian clock feedback loop. Cell 1999;98:193–205

32. Jang H, Lee GY, Selby CP, et al. SREBP1c-CRY1 signalling represses hepatic glucose production by promoting FOXO1 degradation during refeeding. Nat Commun 2016;7:12180

33. Tong X, Buelow K, Guha A, Rausch R, Yin L. USP2a protein deubiquitinates and stabilizes the circadian protein CRY1 in response to inflammatory signals. J Biol Chem 2012;287:25280–25291

34. Bogardus C, Lillioja S, Howard BV, Reaven G, Mott D. Relationships between insulin secretion, insulin action, and fasting plasma glucose concentration in non-diabetic and noninsulin-dependent diabetic subjects. J Clin Invest 1984;74:1238–1246

35. Monnier L, Colette C, Dunseath GJ, Owens DR. The loss of postprandial gly-cemic control precedes stepwise deterioration of fasting with worsening diabetes. Diabetes Care 2007;30:263–269

36. Rizza RA. Pathogenesis of fasting and postprandial hyperglycemia in type 2 diabetes: implications for therapy. Diabetes 2010;59:2697–2707

37. Barclay JL, Shostak A, Leliavski A, et al. High-fat diet-induced hyperinsulinemia and tissue-specific insulin resistance in Cry-deficient mice. Am J Physiol Endocrinol Metab 2013;304:E1053–E1063

38. Shi H, Tzameli I, Bjørbaek C, Flier JS. Suppressor of cytokine signaling 3 is a physiological regulator of adipocyte insulin signaling. J Biol Chem 2004;279:34733–34740

39. Ueki K, Kondo T, Kahn CR. Suppressor of cytokine signaling 1 (SOCS-1) and SOCS-3 cause insulin resistance through inhibition of tyrosine phosphorylation of insulin receptor substrate proteins by discrete mechanisms. Mol Cell Biol 2004;24:5434–5446

40. Hashiramoto A, Yamane T, Tsumiyama K, et al. Mammalian clock gene Cryptochrome regulates arthritis via proinflammatory cytokine TNF-alpha. J Immunol 2010;184:1560–1565

41. Yang L, Chu Y, Wang L, et al. Overexpression of CRY1 protects against the development of atherosclerosis via the TLR/NF-κB pathway. Int Immunopharmacol 2015;28:525–530

42. Moller DE. Potential role of TNF-alpha in the pathogenesis of insulin resistance and type 2 diabetes. Trends Endocrinol Metab 2000;11:212–217

43. Perseghin G, Petersen K, Shulman GI. Cellular mechanism of insulin resistance: potential links with inflammation. Int J Obes Relat Metab Disord 2003;27(Suppl. 3):S6–S11

44. Hirota T, Lee JW, St John PC, et al. Identification of small molecule activators of cryptochrome. Science 2012;337:1094–1097

45. Komander D, Rape M. The ubiquitin code. Annu Rev Biochem 2012;81:203–229

46. Teixeira LK, Reed SI. Ubiquitin ligases and cell cycle control. Annu Rev Biochem 2013;82:387–414

47. Yang XD, Xiang DX, Yang YY. Role of E3 ubiquitin ligases in insulin resistance. Diabetes Obes Metab 2016;18:747–754

48. Song R, Peng W, Zhang Y, et al. Central role of E3 ubiquitin ligase MG53 in insulin resistance and metabolic disorders. Nature 2013;494:375–379

49. Yi JS, Park JS, Ham YM, et al. MG53-induced IRS-1 ubiquitination negatively regulates skeletal myogenesis and insulin signalling. Nat Commun 2013;4:2354

50. Abe T, Hirasaka K, Kagawa S, et al. Cbl-b is a critical regulator of macrophage activation associated with obesity-induced insulin resistance in mice. Diabetes 2013;62:1957–1969

51. Abbas T, Mueller AC, Shibata E, Keaton M, Rossi M, Dutta A. CRL1-FBXO11 promotes Cdt2 ubiquitylation and degradation and regulates Pr-Set7/Set8-mediated cellular migration. Mol Cell 2013;49:1147–1158

52. Rossi M, Duan S, Jeong YT, et al. Regulation of the CRL4(Cdt2) ubiquitin ligase and cell-cycle exit by the SCF(Fbxo11) ubiquitin ligase. Mol Cell 2013;49:1159–1166